A Power-balanced Model of a Valve Exciter Including Shocks and Based on a Conservative Jet for Brass Instruments: Simulations and Comparison with Standard Models

N. Lopes and T. Hélie
IRCAM, 1, place Igor-Stravinsky, 75004 Paris, France
nicolas.lopes@ircam.fr

In most of models of brass instruments (and also of the glottis), the jet is governed by an equation of Bernoulli type (with basic, non stationary or lossy versions). In this exciter part, this model is known to be of first importance because it is responsible for the non-linearity which allows the emergence of self-oscillations. However, this model infringes a fundamental physical property: it does not preserve a well-posed power balance between the reed (possibly lip-reed) and the jet. In particular, the energy stored in the reed is not given back to the jet. In the case of brass instruments and of the glottis, a second similar problem is concerned with shocks, when they are modeled by increasing the values of the mass, damper and spring for negative heights. Indeed, at the contact time, both the kinetic and the potential energies are artificially increased. In this paper, we propose a model of a valve exciter which includes shocks, with a special care to a well-posed power balance: first, the model of the jet is built for basic assumptions; second, a model of shocks is proposed. These models can be recast in the framework of the so-called "port-Hamiltonian systems" which guarantees well-posed power-balance. Finally, simulations (that preserve a discrete-time version of the power balance) are performed for these new models and compared with standard models.

1 Introduction

Many models of brass instruments are available [1, 2]. These systems are known to be self-oscillating, due to the nonlinear coupling involved by the jet between the lips. The movements of the lips operate as a modulator of the aperture, that allows the generation of audible air pulse trains. However, many of the traditionally-used jet models do not properly handle the power exchange between the jet and the lips, in the sense that they discard the transverse component in the velocity field of the jet. Indeed, in this case, the velocity field is unable to transmit a mechanical work in the transverse direction.

In [3], we proposed a well-posed power balanced model of a jet based on a macroscopic representation of an unsteady analytic 2D flow. To this end, we adopted a so-called "*Port-Hamiltonian System*" formalism which guarantees the passivity. This evidenced the kinetic energy of the jet as well as the pumping volumetric flows incurred by the movement of the lips. However, the channel closure and shocks were not included in the model of jet as they represented a particular issue. In this work we propose a way to handle cases of shocks with a power-balanced approach. This paper is organized as follows: In section 2, a simplified model of a brass instrument is presented, and a full explanation of the power issue is done. In section 3, we describe the *Port-Hamiltonian System* (PHS) formalism used in this work, including a proof of the power balance property. Section 4 is devoted to the derivation of models of each organ of the complete instrument under PHS forms. In section 5, a numerical scheme conserving the power balance is proposed as well as a strategy to handle shocks. Finally, in the last section, results obtained from the simulations are discussed.

2 Global description and problem statement

We consider a musician (M) interacting through a jet (J) with an acoustic resonator of the instrument (I). The complete system is idealized and composed of the following seven elementary organs (see figure 1):

(A) Air source: one ideal pressure supply,

(L) Lip: one parallelepipedic mass-spring-damper system,

(F) Flow: one 2D irrotational incompressible flow,

($T_{-,+}$) Turbulences: two generators of losses (T_+ is located downstream at the interface J↔I and T_- is located upstream at the interface M↔J),

(B) Bore: one conservative 1D acoustic straight pipe,

(R) Radiation: one radiation load of resistive type.

The corresponding models are detailed in section 4.

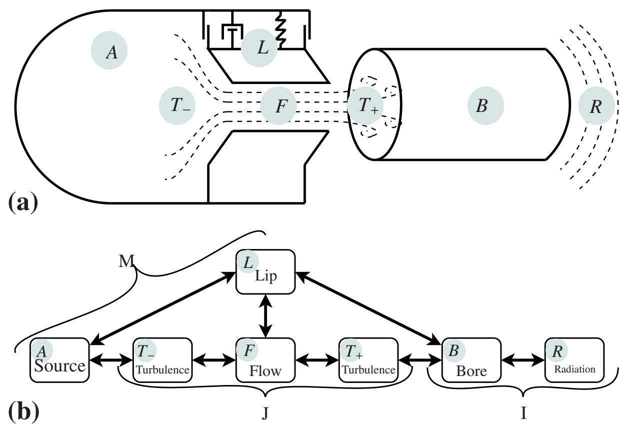

Figure 1: Sketch of the complete system comprised of a musician (M) interacting through a jet (J) with the acoustic resonator of an instrument (I): (a) overview; (b) representation of the power exchanges between elementary organs.

Compared to many models of wind instruments in the literature [4, 5], this work focuses on the design of the non-linearity which is responsible for the self-oscillations, according to two issues: (i) to improve the realism (here, the interaction between the intrument and the player through the jet), and (ii) to guarantee a fundamental physical property (here, the passivity of the jet).

The traditionally-used models of the jet are based on Bernoulli-type equations, for various assumptions on the flow: steady or unsteady cases, and with or without a pumping flow due to the valve movement (see e.g. [6, 7] for a review). In these models, only those that include a pumping volumetric flow can be related to a power balance (see e.g. [8] for the clarinet). However, even in this case, the mechanical work done by the lip on the jet is not properly transfered into the jet, but directly distributed to the acoustic pipe. In [3], we proposed to consider the power exchanges at the boundary between the lip and jet, the state of which is characterized by the fields of pressure and velocity. Under the assumptions on **(F)**, this approach has naturally made the flow of the jet appear as a component that stores kinetic energy. The influence of the kinetic energy (stored in the flow) on the dynamics of the complete system has been evidenced. From a general point of view, these properties of passivity are naturally supported by the formalism of the so-called port-Hamiltonian systems. They are introduced just below.

3 Port-hamiltonian systems: basics and introductory examples

This section provides some introductory elements about Port-Hamiltonian systems [9, 10]. An introduction, similar to that given below, for audio electronic circuits and their simulation can be found in [11].

3.1 Formalism

Consider a physical system composed of (see figure 2a)

- N_S **storage components**: the energy of each component i ($1 \le i \le N_S$) is $\mathcal{E}_i = h_i(x_i) \ge 0$ (typically, for a spring with stiffness k, the state x can be chosen as its stretching length ℓ_{spring}, so that $h(x) = \frac{1}{2}kx^2$);
- N_D **dissipative components**: the dissipative power is $\mathcal{D}_j = r_j(w_j) \ge 0$ (typically, for a viscous damper with coefficient c, the variable w can be chosen as the velocity v_{damper}, so that $r(w) = c.w^2$);
- N_P **external ports**, with incoming power $\mathcal{P}_n$ for each port n.

Denoting efforts e (for example, force, pressure or voltage) and flows f (velocity, volumetric flow or electric current), the power received by a system is given by the product $e.f$, for standard *receiver conventions*. For storage components, these quantities are related to $\frac{\mathrm{d}h_i}{\mathrm{d}x_i}$ and $\frac{\mathrm{d}x_i}{\mathrm{d}t}$ in the sense that the received power is the time variation of the stored energy so that the product $e_i.f_i$ is also $\frac{\mathrm{d}h_i}{\mathrm{d}x_i}.\frac{\mathrm{d}x_i}{\mathrm{d}t} = \frac{\mathrm{d}\mathcal{E}_i}{\mathrm{d}t}$. These relations give the constitutive laws: for a spring the flow $f = \frac{dx}{dt}$ is the velocity v_{spring} and the effort $e = \frac{dh}{dx}(= kx)$ is the force F_{spring}. For dissipative components, a similar mapping is based on the factorization $r_j(w_j) = w_j.z_j(w_j)$: for a damping, the flow $f = w$ is the velocity and the effort $e = d.w = z(w)$ provides the force. For external ports, we arrange efforts e_n and flows f_n in two vectors: one is considered as an input, denoted u_n, and the other one as the associated output, denoted y_n, so that $\mathcal{P}_n = y_n.u_n$.

Given a system with the graph of the connections of its components, physical laws (Newton's laws of motion, Kirchhoff's laws for electronics, etc) provide the relations between all the efforts and the flux. Gathering these relations defines a so-called *Port-Hamiltonian System* (PHS) which, based on the definitions introduced above, appears to be governed by (see [10] for a detailed presentation)

$$\begin{pmatrix} \frac{\mathrm{d}\mathbf{x}}{\mathrm{d}t} \\ \hline \mathbf{w} \\ \hline -\mathbf{y} \end{pmatrix} = \underbrace{\left(\begin{array}{c|c|c} \mathbf{J}_x & -\mathbf{K} & \mathbf{G}_x \\ \hline \mathbf{K}^T & \mathbf{J}_\omega & \mathbf{G}_w \\ \hline -\mathbf{G}_x^T & -\mathbf{G}_w^T & \mathbf{J}_y \end{array}\right)}_{\mathbf{S}} . \begin{pmatrix} \nabla\mathcal{H}(x) \\ \hline \mathbf{z(w)} \\ \hline \mathbf{u} \end{pmatrix}, \quad (1)$$

where matrices $\mathbf{J}_x$, $\mathbf{J}_w$, $\mathbf{J}_y$ (and so $\mathbf{S}$) are skew-symmetric. Function $\nabla\mathcal{H} : \mathbb{R}^{N_S} \to \mathbb{R}^{N_S}$ denotes the gradient of the total energy $\mathcal{E} = \mathcal{H}(\mathbf{x}) = \sum_{i=1}^{N_S} h_i(x_i)$ w.r.t. the state $\mathbf{x} = [x_1, \ldots, x_{N_S}]^T$. Function $\mathbf{z} : \mathbb{R}^{N_D} \to \mathbb{R}^{N_D}$ denotes the collection of functions z_j w.r.t. the vector $\mathbf{w} \in \mathbb{R}^{n_D}$ so that the total dissipated power is $\mathcal{D} = \mathbf{z}(\mathbf{w})^T.\mathbf{w} = \sum_{j=1}^{N_D} r_j(w_j)$. The incoming power is $\mathcal{P} = \mathbf{u}^T.\mathbf{y}$ where $\mathbf{u} = [u_1, \ldots, u_{N_P}]^T$ and $\mathbf{y} = [y_1, \ldots, y_{N_P}]^T$ are the inputs and the outputs corresponding to external ports.

Property 1 (Passivity) *The time variation of the total energy $\mathcal{E} = \mathcal{H}(\boldsymbol{x})$ is*

$$\frac{\mathrm{d}\mathcal{E}}{\mathrm{d}t} = -\mathcal{D} + \mathcal{P} \quad (2)$$

Proof: Rewrite (1) as $\mathbf{B} = \mathbf{S}.\mathbf{A}$. As S is skew-symmetric, $0 = \mathbf{A}^T.\mathbf{S}.\mathbf{A} = \mathbf{A}^T.\mathbf{B} = \nabla\mathcal{H}(x)^T.\frac{\mathrm{d}\mathbf{X}}{\mathrm{d}t} + \mathbf{z}(\mathbf{w})^T.\mathbf{w} - \mathbf{u}^T.\mathbf{y} = \frac{\mathrm{d}\mathcal{E}}{\mathrm{d}t} + \mathcal{D} - \mathcal{P}$.

3.2 Example: a mass-damper-spring system

Consider the mechanical system composed of:

- $N_S = 2$ **storage components**: first, a solid with mass m (we choose here the state x_1 as the momentum $\mathfrak{p}_{\text{mass}} = m.v_{\text{mass}}$, with kinetic energy $h_1(x_1) = \frac{1}{2m}x_1^2$); second, a spring with stiffness k as in § 3.1 ($x_2 = \ell_{\text{spring}}$ and $h_2(x_2) = \frac{1}{2}kx_2^2$);
- $N_d = 1$ **dissipative component**: a damper with coefficient c as in § 3.1 ($w_1 = v_{\text{damper}}$ and $D_1(w_1) = c.w_1^2$);
- $N_P = 1$ **external port**: we choose the input u_1 as the external force F_{ext} applied to the solid so that the output y_1 is the power-complentary quantity, that is, the velocity v_{ext} associated to the port.

Now that theses definitions are introduced, independently of each other, we consider the graph of the connections of the complete system described in figure 2. The total energy is $\mathcal{E} = \mathcal{H}(\mathbf{x}) = h_1(x_1) + h_2(x_2)$, the total internal dissipated power is $\mathcal{D} = r_1(w_1)$ and the total external incoming power is $\mathcal{P} = y_1.u_1$.

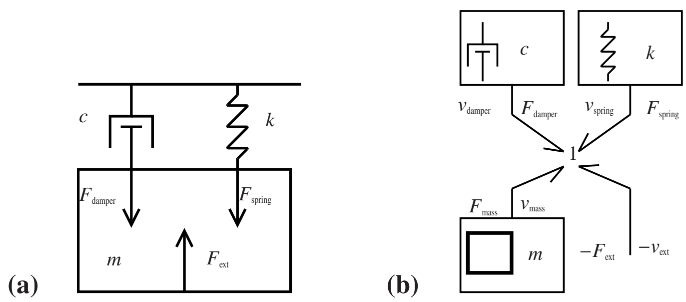

Figure 2: (a) Mass-spring-damper system subjected to an external force (with no gravity field). (b) Bond graph representation of the system

For this system, the left-hand side of (1) is $\mathbf{B} = \left[\frac{\mathrm{d}x_1}{\mathrm{d}t}, \frac{\mathrm{d}x_2}{\mathrm{d}t}, w_1, -y_1\right]^T$. It corresponds to the physical quantities $\left[F_{\text{mass}}, v_{\text{spring}}, v_{\text{damper}}, -v_{\text{ext}}\right]^T$, where $F_{\text{mass}} = \frac{\mathrm{d}\mathfrak{p}_{\text{mass}}}{\mathrm{d}t}$ and $v_{\text{spring}} = \frac{\mathrm{d}\ell_{\text{spring}}}{\mathrm{d}t}$. The vector on the right-side is $\mathbf{A} = \left[\partial_{x_1}\mathcal{H}(\mathbf{x}), \partial_{x_2}\mathcal{H}(\mathbf{x}), z_1(w_1), u_1\right]^T$, where $z_1(w_1) =$

$r_1(w_1)/w_1$ is introduced in § 3.1. Its derivation yields the power-complementary quantities of $\mathbf{B}$ given by $\left[v_{\text{mass}}, F_{\text{spring}}, F_{\text{damper}}, F_{\text{ext}}\right]^T$, where $F_{\text{spring}} = k\ell_{\text{spring}}$ and $F_{\text{damper}} = cv_{\text{damper}}$.

From the physical laws, the relations between these two vectors are

$$\begin{pmatrix} F_{\text{mass}} \\ \hline v_{\text{spring}} \\ \hline v_{\text{damper}} \\ \hline -v_{\text{ext}} \end{pmatrix} = \left(\begin{array}{cc|c|c} 0 & -1 & -1 & 1 \\ 1 & 0 & 0 & 0 \\ \hline 1 & 0 & 0 & 0 \\ \hline -1 & 0 & 0 & 0 \end{array}\right) \cdot \begin{pmatrix} v_{\text{mass}} \\ \hline F_{\text{spring}} \\ \hline F_{\text{damper}} \\ \hline F_{\text{ext}} \end{pmatrix}. \tag{3}$$

This equation restores the form (1), block by block.

4 Physical models and representation into PHS forms

This section provides a description of each organ introduced in §2.

4.1 Musician (M)

4.1.1 Air Supply (A)

The air supply is the only active element of the system. In this article, we consider that the air pressure supply is ideal (P_A). The power consumed by the system is $\mathcal{P}_A(t) = P_A(t)U_A(t)$ where U_A is the power-complementary quantity, in this case, a volumetric flow.

4.1.2 Lip (L)

The lip (L) is modeled as a mass-spring-damper system presented in figure 3.

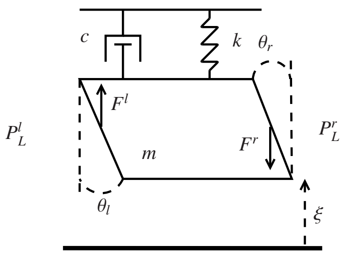

Figure 3: Model of a simplified lip (L).

We use the model described in the example § 3.2 with the choice of variable $\left[\dot{\xi}, \xi\right]^T$. Using the velocity instead of the momentum as a state makes the matrix S_L dependent of the mass m but will simplify the connection. Forces applied on left and right surfaces are $F^l_L = S_l P^l_L$ and $F^r_L = S_r P^r_L$ with $S_l = A_l sin(\theta_l)$ and $S_r = A_r sin(\theta_r)$ (see figure 3). Introducing $\mathbf{x}_L = \left[\dot{\xi}, \xi\right]^T$, $\mathbf{w}_L = \left[w_L\right]$, $\mathbf{u}_L = \left[F_L, P^l_L, P^r_L\right]^T$, $\mathbf{y} = \left[V_L, U^l_L, U^r_L\right]^T$,(L) can be formulated into a PHS (1) where the skew-symmetric matrix S_L is :

$$S_L = \left(\begin{array}{cc|c|ccc} 0 & -1/m & -1/m & 1/m & S_l/m & -S_r/m \\ 1/m & 0 & 0 & 0 & 0 & 0 \\ \hline 1/m & 0 & 0 & 0 & 0 & 0 \\ \hline -1/m & 0 & 0 & 0 & 0 & 0 \\ -S_l/m & 0 & 0 & 0 & 0 & 0 \\ S_r/m & 0 & 0 & 0 & 0 & 0 \end{array}\right).$$

The energy of the system (L) is $\mathcal{E}_L = \mathcal{H}_L(\mathbf{x}_L) = \frac{1}{2}m\dot{\xi}^2 + \frac{1}{2}k(\xi - \xi_0)^2$ where ξ_0 denotes the equilibrium position.

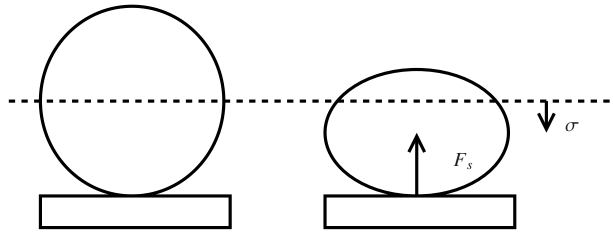

Figure 4: Illustration of a Hertz-type shock: σ denotes the crushing of the lip and F_s is the resulting force.

When the channel is closed ($\xi < 0$), we consider the crushing of the lip $\sigma \geq 0$. In this paper, the non-linear Hertz model of shock is used and discribes the energy stored during a shock as $\mathcal{H}_s(\sigma) = \frac{2}{5}\alpha\sigma^{\frac{5}{2}}$. The dissipated power is linear and represented by a damper with coefficient "β" ($w_s = \dot{\sigma}$ and $D_s(\dot{\sigma}) = \beta\dot{\sigma}^2$). Thus, introducing $\mathbf{x}_L = \left[\dot{\xi}, \xi, \sigma\right]^T$, $\mathbf{w}_L = \left[w_L, w_s\right]$, $\mathbf{u}_L = \left[F_L, P^l_L, P^r_L\right]^T$, $\mathbf{y} = \left[V_L, U^l_L, U^r_L\right]^T$,(L) can be reformulated, including shocks, into a PHS (1) where the new skew-symmetric matrix S_L is :

$$S_L = \left(\begin{array}{ccc|cc|ccc} 0 & -1/m & K_s/m & 1/m & K_s/m & 1/m & S_l/m & -S_r/m \\ 1/m & 0 & 0 & 0 & 0 & 0 & 0 & 0 \\ -K_s/m & 0 & 0 & 0 & 0 & 0 & 0 & 0 \\ \hline 1/m & 0 & 0 & 0 & 0 & 0 & 0 & 0 \\ -K_s/m & 0 & 0 & 0 & 0 & 0 & 0 & 0 \\ \hline -1/m & 0 & 0 & 0 & 0 & 0 & 0 & 0 \\ -S_l/m & 0 & 0 & 0 & 0 & 0 & 0 & 0 \\ S_r/m & 0 & 0 & 0 & 0 & 0 & 0 & 0 \end{array}\right),$$

where $K_s = 0$ when the channel is open and $K_s = 1$ during the contact. The total energy of the system (L) is $\mathcal{E}_L = \mathcal{H}_L(\mathbf{x}_L) = \frac{1}{2}m\dot{\xi}^2 + \frac{1}{2}k(\xi - \xi_0)^2 + \mathcal{H}_s(\sigma)$.

4.2 Jet (J)

The jet is composed of a flow (under the lip) and a dissipation by turbulence. Turbulences can be activated upstream and downstream the flow.

4.2.1 Flow (F) and macroscopic form

We consider an irrotationnal 2D flow of an incompressible perfect fluid in a time-varying volume $\Omega(t) = \ell\zeta\xi(t)$ where ℓ and ζ denote the length and the width of the channel respectively. This flow is contained between a static wall (at bottom) and a mobile wall (at the top), so that the transverse velocities are uniform on these boundaries (see figure 5). For sake of simplicity, the longitudinal velocities are also chosen to be uniform on the left and right boundaries: this assumption makes the corresponding airflows be the product of these velocities by the areas of the boundaries.

Neglecting the effect of the gravity, velocity and pressure fields are governed by

$$\nabla \times \mathbf{v} = 0, \tag{4}$$

$$\nabla.\mathbf{v} = 0, \tag{5}$$

$$\frac{\mathrm{d}\mathbf{v}}{\mathrm{d}t} + \nabla(\frac{|\mathbf{v}|^2}{2}) + \frac{1}{\rho_0}\nabla(p) = 0, \tag{6}$$

inside the domain where ρ_0 is the air density, and by $v_y(x, y = 0, t) = 0$ and $v_y(x, y = \xi, t) = \dot{\xi}(t)$ for all $x \in [0, \ell]$ at the bottom and top boundaries.

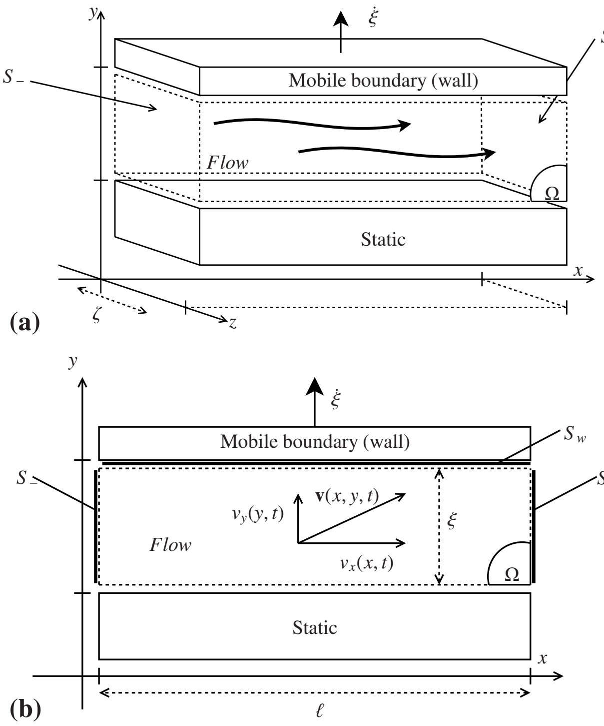

Figure 5: 2D irrotationnal flow under a mobile wall (invariant along the axis z): the velocity field $\mathbf{v}(x, y, t) = v_x(x, y, t)\mathbf{e}_x + v_y(x, y, t)\mathbf{e}_y$.

The general solution for uniform longitudinal velocities v_x at the left and right boundaries is given by (see e.g. [12, § 5.5])

$$\begin{cases} v_x(x, y, t) &= v_0(t) - \frac{\dot{\xi}}{\xi}x \\ v_y(x, y, t) &= \frac{\dot{\xi}}{\xi}y, \end{cases} \tag{7}$$

and

$$p(x, y, t) = p_0(t) + \rho_0\left[\frac{1}{2}(x^2 - y^2)\frac{\ddot{\xi}}{\xi} - x^2\frac{\dot{\xi}^2}{\xi^2} - \left(\dot{v}_0 - \frac{\dot{\xi}}{\xi}v_0\right)x\right], \tag{8}$$

where $v_0(t)$ denotes the longitudinal velocity at the left boundary and $p_0(t)$ denotes the pressure at the left bottom corner. In [3], it has been shown that the model of flow can be reduced to an equivalent macroscopic description with average variables (on the volume for the state variables and on the control surfaces for the external port variables). We found that the macroscopic model corresponds to a PHS described by the differential system under the form (1) with:

$$\begin{aligned} \mathbf{x}_F &= \left[\langle v_x\rangle_\Omega, \langle v_y\rangle_\Omega, \xi\right]^T = \left[V_x, V_y, \xi\right]^T && (9)\\ \mathbf{u}_F &= \left[\langle p + \frac{1}{2}\rho|\mathbf{v}|^2\rangle_{S_-}, \langle p + \frac{1}{2}\rho|\mathbf{v}|^2\rangle_{S_+}, S_w\langle p\rangle_{S_w}\right]^T && (10)\\ &= \left[P_F^-, P_F^+, F_F\right]^T && (11)\\ \mathbf{y}_F &= \left[S_-v_x(0, t), -S_+v_x(l, t), -\dot{\xi}\right]^T && (12)\\ &= \left[U_F^-, U_F^+, V_F\right]^T && (13) \end{aligned}$$

$$S_F = (1 - K_c)\left(\begin{array}{ccc|ccc} 0 & 0 & 0 & \frac{\zeta\xi}{\eta} & -\frac{\zeta\xi}{\eta} & 0 \\ 0 & 0 & -\frac{2}{\eta\alpha} & \frac{\zeta l}{\eta\alpha} & \frac{\zeta l}{\eta\alpha} & -\frac{2}{\eta\alpha} \\ 0 & \frac{2}{\eta\alpha} & 0 & 0 & 0 & 0 \\ \hline -\frac{\zeta\xi}{\eta} & -\frac{\zeta l}{\eta\alpha} & 0 & 0 & 0 & 0 \\ \frac{\zeta\xi}{\eta} & -\frac{\zeta l}{\eta\alpha} & 0 & 0 & 0 & 0 \\ 0 & \frac{2}{\eta\alpha} & 0 & 0 & 0 & 0 \end{array}\right)$$

and $\mathcal{H}_F(\mathbf{x}_F) = \frac{1}{2}\eta(\xi)V_x^2 + \frac{1}{2}\eta(\xi)\alpha(\xi)V_y^2$. Where, $\langle f\rangle_A(t) = \frac{1}{A}\int_A f(x, y, t)dA$ denotes the average of a quantity $f(x, y, t)$ over a surface or a volume A.

Remark 1 (Closed channel) *This model is not defined when $\xi = 0$. In this work, we choose to considere a closed channel when $\xi = \epsilon \ll 1$. When the channel is closed, $K_s = 0$ and $V_x = V_y = 0$.*

4.2.2 Viscous losses: Poiseuille's model

At this point a simple model of viscous losses can be added using a Poiseuille's model.

$$v_x(x, y, t) = v_{max}\left(\frac{4y}{\xi} - \frac{4y^2}{\xi^2}\right)$$

$$V_x(t) = \langle v_x(x, y, t)\rangle_\Omega = \frac{2}{3}v_{max}$$

The total dissipated power w.r.t. the state variable V_x in the flow is:

$$\begin{aligned} D_\nu(V_x) &= -\int_\Omega \rho v_x(x, y, t)\nu\partial_y^2 v_x(x, y, t)\partial_\Omega && (14)\\ &= 12\nu\rho\frac{l\zeta}{\xi}V_x^2 && (15)\\ &= w_\nu z_\nu(w_\nu) && (16) \end{aligned}$$

where $w_\nu = V_x$, $z_\nu(w_\nu) = 12\nu\rho\frac{l\zeta}{\xi}V_x$ and ν is the kinetic viscosity. Thereby, the viscous losses can be considered as a dissipative component which can be added to the flow model (F).

4.2.3 Turbulences ($\mathbf{T}_{+,-}$)

Numerous experimental studies on model profiles of vocal cords or lips emphasize that, at the end of the channel (here, under a lip with an ideal geometry), the flow is separated from the walls to form a jet and vortices. These vortices may progressively disintegrate until appearance of turbulences. This complexity is often simplified introducing a dissipation of the kinetic energy of the jet [13]. We consider such a dissipative model (here, total): One (T_+) upstream for a positive volumetric flow, and one (T_-) downstream for a negative volumetric flow. Thereby, we can easily write the dissipated energy as:

$$\begin{aligned} \langle\frac{1}{2}\rho|\mathbf{v}|^2\rangle_{S_-} &= \frac{1}{2}\rho\frac{U_F^{-2}}{\xi^2\zeta^2} + \frac{1}{2}\rho\frac{4}{3}V_y^2 \\ \langle\frac{1}{2}\rho|\mathbf{v}|^2\rangle_{S_+} &= \frac{1}{2}\rho\frac{U_F^{+2}}{\xi^2\zeta^2} + \frac{1}{2}\rho\frac{4}{3}V_y^2 \end{aligned}$$

Remark 2 (Bernoulli-type turbulences) *The second term of the kinetic energy is due to the transverse velocity in the flow. It is not included in 1D classical models.*

Denoting, $w_- = -U_F^-$ and $w_+ = -U_F^+$, one can define the upstream and downstream dissipated power by:

$$\begin{aligned} \mathcal{P}_T &= w.\left(\frac{1}{2}\rho\frac{w^2}{\xi^2\zeta^2} + \frac{1}{2}\rho\frac{4}{3}V_y^2\right) \quad if\ w > 0 \\ &= 0 \quad if\ not. \end{aligned}$$

We define the functions of dissipation (T_+) and (T_-) by:

$$z_T(w) = (\frac{1}{2}\rho\frac{w^2}{\xi^2\zeta^2} + \frac{1}{2}\rho\frac{4}{3}V_y^2)\Phi(w)$$

where $\Phi(w)$ is a phenomenological function such that $w.z_T(w) > 0 \ \ \forall\, w \in \mathbb{R}$, $w.z_T(w) \ll 1 \ \ \forall\, w \leq 0$ such that $\frac{dz_T}{dw}(0)$ is defined.

4.3 Instrument (I)

In this work, we use the instrument part presented in [3] in which we consider the linear acoustic propagation of plane waves in a lossless bore with a section s_0 and a lenght L_0. The radiation at the exit of the tube is modeled by a load of resistive type $p(L,t) = Z_L u(L,t)$ with real passive impedance $Z_L > 0$.

5 Simulation

5.1 Numeric scheme preserving the power balance

5.1.1 Principle

A temporal pattern is applied to the energy to calculate its discrete version. Then, to maintain the power balance of our system, we write this variation as a function of the variation of the state: in other words, we provide the differentiation of the composition of two functions. $d\mathcal{E}(t,dt) = \dot{\mathcal{E}}(t)dt$ becomes $\delta\mathcal{E}(t,\delta t) = \mathcal{E}(t+\delta t) - \mathcal{E}(t)$ and $\partial_t\mathcal{E} = \partial_t\mathcal{H}(\mathbf{x}) = \nabla_{\mathbf{x}}\mathcal{H}^T.\partial_t\mathbf{x}$ becomes $\delta\mathcal{H}(t,\delta t) = \partial^d_{\mathbf{x}}\mathcal{H}(\mathbf{x},\delta\mathbf{x})^T.\delta\mathbf{x}(t,\delta t)$. Introducing the discrete gradient $\partial^d_{\mathbf{x}}\mathcal{H}(\mathbf{x},\delta\mathbf{x})$, we achieve a time discretization informed by the physical parameters of the system.

The discrete version of the PHS is obtained by replacing the time derivative and the gradient by their discrete versions. The discrete power balance follows directly from the skew-symmetric matrix S. In the general case, the solution of the discrete gradient is not unique. However, one can define a unique symmetric version as the average of all possible versions.

5.1.2 Basic example

Applying this method to the mass-spring-damper system presented in the example §2.2, we have: $\partial^d_{\mathbf{x}}\mathcal{H}(\mathbf{x},\delta\mathbf{x}) = \frac{1}{2}([\partial^d_{\mathbf{x}}\mathcal{H}(\mathbf{x},\delta\mathbf{x})]_1 + [\partial^d_{\mathbf{x}}\mathcal{H}(\mathbf{x},\delta\mathbf{x})]_2)$ with

$$[\partial^d_{\mathbf{x}}\mathcal{H}(\mathbf{x},\delta\mathbf{x})]_1 = \begin{pmatrix} \frac{\mathcal{H}(x_1+\delta x_1, x_2+\delta x_2) - \mathcal{H}(x_1, x_2+\delta x_2)}{\delta x_1} \\ \frac{\mathcal{H}(x_1, x_2+\delta x_2) - \mathcal{H}(x_1, x_2)}{\delta x_2} \end{pmatrix}$$

$$[\partial^d_{\mathbf{x}}\mathcal{H}(\mathbf{x},\delta\mathbf{x})]_2 = \begin{pmatrix} \frac{\mathcal{H}(x_1+\delta x_1, x_2) - \mathcal{H}(x_1, x_2)}{\delta x_1} \\ \frac{\mathcal{H}(x_1, x_2+\delta x_2) - \mathcal{H}(x_1, x_2)}{\delta x_2} \end{pmatrix}$$

Finally,

$$\partial^d_{\mathbf{x}}\mathcal{H}(\mathbf{x},\delta\mathbf{x}) = \begin{pmatrix} \frac{1}{m}x_1 + \frac{1}{2m}\delta x_1 \\ kx_2 + \frac{1}{2}k\delta x_2 \end{pmatrix} \tag{17}$$

$$= \nabla_X\mathcal{H}(\mathbf{x}) + \frac{1}{2}\begin{pmatrix} \frac{1}{m} & 0 \\ 0 & k \end{pmatrix}\begin{pmatrix} \delta x_1 \\ \delta x_2 \end{pmatrix}. \tag{18}$$

The discrete scheme is informed by the physical parameters m and k, and the discrete PHS is:

$$\begin{pmatrix} \frac{\delta x_1}{\delta t} \\ \frac{\delta x_2}{\delta t} \\ \hline w_1 \\ \hline -y \end{pmatrix} = \left(\begin{array}{cc|c|c} 0 & -1 & -1 & 1 \\ 1 & 0 & 0 & 0 \\ \hline 1 & 0 & 0 & 0 \\ \hline -1 & 0 & 0 & 0 \end{array}\right) \cdot \begin{pmatrix} \partial^d_{x_1}\mathcal{H}(\mathbf{x},\delta\mathbf{x}) \\ \partial^d_{x_2}\mathcal{H}(\mathbf{x},\delta\mathbf{x}) \\ \hline z_1(w_1) \\ \hline u \end{pmatrix}.$$

5.2 Simulation method and shocks

For a sampling period $\delta t = 1/f_s$, the discrete PHS version leads to solve equations involving $\delta X(t_k,\delta t)$ and $w(t_k)$ (for known $x(t_k)$ and $u(t_k)$). We can thus deduce $x(t_{k+1}) = x(t_k) + \delta x(t_k,\delta t)$ and $y(t_{k+1})$. In practice, implicit relations are solved using a Newton-Raphson type algorithm. For this article, the sampling frequency is $192000Hz$. Shocks are handled following steps illustrated in figure (6). Considering an opened channel $K_s = 0$, if $\xi(t_k) + \delta\xi(t_k,\delta t) < \epsilon$, δt_{shock} is calculated to have $\xi(t_{shock}) = \xi(t_k) + \delta\xi(t_k,\delta t_{shock}) = \epsilon$. Then, the next step is calculated with $\xi(t_{k+1}) = \xi(t_{shock}) + \delta\xi(t_{shock},\delta t)$ and $K_s = 1$. Next steps are computed with $K_s = 1$ until $\xi(t_k) + \delta\xi(t_k,\delta t) > \epsilon$. Then, δt_{shock} is calculated to have $\xi(t_{shock}) = \xi(t_k) + \delta\xi(t_k,\delta t_{shock}) = \epsilon$. Finally, the next step is calculated with $\xi(t_{k+1}) = \xi(t_{shock}) + \delta\xi(t_{shock},\delta t)$ and $K_s = 0$.

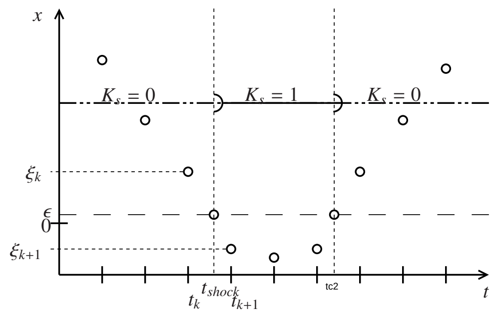

Figure 6: Illustration of the strategy to handle shocks

6 Results

6.1 Issues and first solutions

The connection between organs is done following the method exposed in [3]. First simulations showed two main issues concerning shocks.

Channel closure: $K_{shock} = 0 \rightarrow 1$

At the channel closure, an incompressible amount of fluid must be quickly expelled such as the force applied by the fluid on the lip becomes high. In such circumstances, the Newton Raphson algorithm does not converge on a solution. A temporary solution is to artificially decrease the channel length.

Channel opening: $K_{shock} = 1 \rightarrow 0$

At the channel opening, a discontinuity is created at the flow inputs. This causes a peak of the longitudinal speed of the fluid V_x. In such circumstances, the Newton Raphson algorithm does not converge on a solution. To cope with this limitation, the dissipative component based on the

Poiseuille's model and presented in 4.2.2 is added to the model of flow.

6.2 First results and discussion

Simulations are done for two models: ($\mathcal{M}_{2D}$) is the 2D model presented in this work, ($\mathcal{M}_{1D}$) is the Bernoulli-type model included pumping flows. Simulation parameters are based on the geometry of the trombone and are given in table 1.

Quantity	Label	Units	Values
Lip thickness/ Channel length	l	m	0.004
Lip length	ζ	m	0.025
Lip surfaces (left/right)	S_l/S_r	m^2	0.000176
Equilibrium position	ξ_0	m	-0.001
Mass of the lip	m	Kg	0.0015
Damper coefficient	c	Ns/m	0.161
Natural frequency		Hz	85.5
Supply air pressure	P_A	Pa	8000.
Tube radius		m	0.025
Tube length	L	m	1
Radiation coefficient	λ		-0.9
kinematic viscosity	ν	m^2/s	1.5610^{-5}

Table 1: Parameters for the experiment.

Results are presented in figure 7. We can see that the system is self-oscillating. Moreover, in this particular configuration, both models behave similarly.

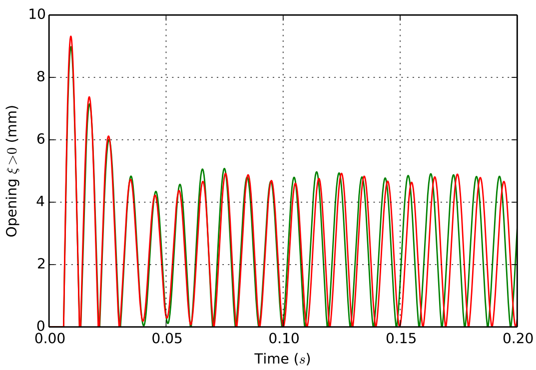

Figure 7: Experiment: Curves: (Green-$\mathcal{M}_{1D}$), (Red-$\mathcal{M}_{2D}$). Opening of the channel ξ w.r.t the time

In other configurations, one could show that the solution for the channel closure ($K_s : 0 \rightarrow 1$) is not efficient to compute the Newton Raphson algorhytm. Anyway, this solution does not verify the power balance as a parameter of the system is artificially modified.

7 Conclusion and perspectives

In this work, we have presented a model of shock compatible with the model of flow previously given in [3]. We proposed a strategy for simulations. However, we saw that the simulation strategy is limited by the Newton Raphson algorithm.

A solution is currently developed to compute simulations without Newton-Raphson type algorithm. This future work will include a model of viscous losses in the flow. It will not be based on a Poiseuille's model which is not enough realistic for such an unsteady flow, but on a boundary layer model. In addition, a second lip model will permit studies to be done on double-reed instruments as well as vocal cords. Finally, an experimental study on artificial mouth [14] will be led. In this context, this model will be approached with a control point of view using the energy as a candidate for Lyapunov function.

Acknowledgment

The authors wish to thank the HAMECMOPSYS ANR projects.

References

[1] C. Vergez. *Trompette et Trompettiste: un systčme dynamique non linéaire analysé, modélisé et simulé dans un contexte musical.* Thčse de doctorat, Ircam, Paris, 2000.

[2] M. V. Walstijn. *Discrete-time modeling of brass and reed woodwind instruments with application to musical sound synthesis*. Phd, University of Edinburgh, United Kingdom, 2002.

[3] T. Hélie N. Lopes. Modèle d'interaction jet/lèvre préservant le bilan de puissance pour les instruments de type cuivre. *Congrès Français d'Acoustique*, 2014.

[4] J. Kergomard A. Chaigne. *Acoustique Des Instruments De Musique (The Physics of Musical Instruments).* Echelles edition, 2008.

[5] T. Rossing N. Fletcher. *The Physics of Musical Instruments*. Springer-Verlag, 1998.

[6] C. Vergez and X. Rodet. Air flow related improvements for basic physical models of brass instruments. In *ICMC: International Computer Music Conference*, Berlin, Allemagne, Septembre 2000.

[7] Deverge M., Pelorson X., Vilain C., Lagrée P.-Y.-L., Chentouf F., Willems J., and Hirschberg A. Influence of the collision on the flow through in-vitro rigid models of the vocal folds. *J. Acoust. Soc. Am.*, 114(6), 2003.

[8] S. Bilbao. Direct simulation for wind instrument synthesis. In *Conference on Digital Audio Effects*, 2008.

[9] A. van der Schaft. Port-hamiltonian systems: an introductory survey. In *Proceedings of the International Congress of Mathematicians*, pages 1339–1365, 2006.

[10] S. Stramigioli H. Bruyninckx V. Duindam, A. Macchelli. *Modeling and Control of Complex Physical Systems: The Port-Hamiltonian Approach*. Springer, 2009.

[11] A. Falaize-Skrzek. Simulation of an analog circuit of a wah pedal: a port-hamiltonian approach. In *Audio Engineering Society, Convention Paper*, 2013.

[12] L. Ryhming. *Dynamique des fluides: un cours de base du deuxičme cycle universitaire*. Presses Polytechniques Romandes, 2004.

[13] A. Hirschberg. Musical aero-acoustics of the clarinet. In *Journal de physique*, volume 4, 1995.

[14] N. Lopes. Control of an artificial mouth playing a trombone and analysis of sound descriptors on experimental data. In *Stockholm Music Acoustics Conference*, 2013.